VILNIUS TECH
Vilnius Gediminas Technical University

Geodesy and Cartography
ISSN 2029-6991 / eISSN 2029-7009
2022 Volume 48 Issue 3: 170–176
https://doi.org/10.3846/gac.2022.14644

UDC 528.8

DUAL-CHANNEL MODEL FOR SHALLOW WATER DEPTH RETRIEVAL FROM WORLDVIEW-3 IMAGERY A CASE STUDY OF KARIMUNJAWA WATERS, CENTRAL JAVA, INDONESIA

Abdul BASITH[1], Luhur Moekti PRAYOGO[1*], Gathot WINARSO[2], Kuncoro Teguh SETIAWAN[2]

[1]*Department of Geodetic Engineering, Faculty of Engineering, Universitas Gadjah Mada, Jl. Grafika No. 2, Yogyakarta, 55281, Indonesia*
[2]*Remote Sensing Application Center, Indonesian National Institute of Aeronautics and Space, BRIN, Jln. Kalisari No. 8 Pekayon, 13710 Pasar Rebo, Jakarta, Indonesia*

Received 26 March 2021; accepted 02 September 2022

Abstract. This research aims to estimate shallow water depth using Worldview 3 satellite imagery and dual-channel models in Karimunjawa waters, Central Java – Indonesia. To build dual-channel models, we used spectral data that had been validated in the field. Twenty-three depth data were recorded synchronous to the spectral data used in forming the semi-analytical dual-channel models. Twelve models were tested using 633 depth data with a non-linear model using multiple polynomial regression analysis degrees 1 and 2. This research has shown that the proposed model has been confirmed to improve depth accuracy. Models using blue and green channels of Worldview 3 image result in good accuracies especially for estimating depths with interval from 5 to 20 meters with RMSE of 1,592 meters (5–10 meters), 2,099 meters (10–15 meters), and 1,239 meters (15–20 meters). The wavelengths of two channels have a low absorption rate to penetrate deeper waters than other wavelengths. The research also finds out that there are still models that meet the IHO standard criteria.

Keywords: satellite-derived bathymetry, water physical properties, spectral field, Worldview 3, Karimunjawa.

Introduction

Integrated coastal management requires a variety of hydrographic information such as bathymetry, currents, waves and tides in order to make it optimal and effective in its management. Such management is essential because most industries are located in coastal areas. As a result, the areas experience reasonably fast economic growth (Hidayah et al., 2018). In coastal management, the need for water depth information (bathymetry) is critical (Prayogo & Basith, 2020) because the data can be used for various purposes in hydrography, such as coastal engineering and shipping trajectory (Gao, 2009; Jupp, 1989; Leu & Chang, 2005).

A trend of passive remote sensing can provide water depth information using the *Satellite-Derived Bathymetry* (SDB) technique (Karimi et al., 2016; Lyzenga, 1985; Stumpf et al., 2003a). SDB is a remote sensing technique that is often used in marine field to obtain the depth information of seas or oceans. This technique is carried out by using satellite imagery by correlating the measured depth with the surface reflectance of the image (Benny & Dawson, 1983; Bierwirth et al., 1993; Collet et al., 2000; Garlan, 1989; Lyzenga, 1978; Provost et al., 1999; Sánchez-Carnero et al., 2014; Sutherland et al., 2004) using the single or quasi-single scattering theory (Sánchez-Carnero et al., 2014).

In its application, marine remote sensing technology cannot be separated from the propagation of electromagnetic energy that enters the water column (Danoedoro, 2012). This energy will be absorbed by the water column's optical properties, which are influenced by the water's material and the angle of incidence of light. This phenomenon will cause electromagnetic waves to hit the water column. Consequently, the waves will be scattered or absorbed, so-called attenuation (Misra et al., 2018). Attenuation causes electromagnetic waves to experience many interactions when received by satellite sensors. The interactions also make light intensity in the water column decrease exponentially. Further, the attenuation process causes light penetration to have different abilities in penetrating the water column. Thus, attenuation is needed to

*Corresponding author. E-mail: *abd_basith@ugm.ac.id*

determine the waters' characteristics (Misra et al., 2018).

The visible remote sensing is a remote sensing technique that uses visible waves in its application (Martin, 2014). Visible rays can penetrate the water column quite well that is connected with marine remote sensing or well-known as marine optics. Marine optics are the optical properties of marine waters, which are used as the basis to develop marine remote sensing.

Nowadays, the trend of using dual-channel in the SDB technique focuses on empirical methods. This method relies on the relationship between the spectral value in the image and the measured depth, band ratios with different wavelengths (Bramante et al., 2013; Dierssen et al., 2003; Sánchez-Carnero et al., 2014; Stumpf et al., 2003b), and the application of the Lyzenga algorithm (Sánchez-Carnero et al., 2014; Sutherland et al., 2004). This method is widely used to estimate sea depth.

Nevertheless, new research using dual-channel algorithms needs to be carried out, especially those that utilize methods other than empirical methods. This research then chooses to use a semi-analytical method. The semi-analytical model formed using the field size's surface reflectance and measured depth data were then applied to estimate the depth in the image. One of the consideration is because the satellite sensors that record water surface objects is not the same as when measuring the physical properties of water in the field to produce different values (Lafon et al., 2002). These conditions allow the SDB analysis to use the semi-analytical method.

Therefore, this research aims to estimate shallow water depth using dual-channel and field parameters, known as the SDB semi-analytical method in Karimunjawa waters, Central Java, Indonesia. Dual-channel is chosen because it will support each other in estimating waters where weak channels with high absorption will be covered with solid channels with low absorption rates.

1. Materials and methods

1.1. Materials

1.1.1. Worldview-3 imagery

In this research, Worldview-3 imagery was acquired on February 21, 2018, calibrated by AComp Radiometric, Level ORStandart2A. According to Basith and Prastyani (2020), the AComp correction produced a better depth estimation than the QUAC and FLAASH radiometric corrections. The Worldview-3 had a spatial resolution of 31 centimeters on the Panchromatic Band and 1.24 meters on the Multispectral Band. The *Ground Sampling Distance* (GSD) generated from this image was 1 meter <1.0 day. The imagery had a high revisit time capability of 4.5 days at 20o off-nadir. Bands in this image were divided into three groups "Panchromatic, Multispectral, and SWIR". Table 1 shows the wavelength specification in the Worldview 3 imagery:

Table 1. Worldview-3 imagery specifications (source: Satellite Imaging Corporation, 2020)

Primary Use/ Band	Wavelength (nm)
Panchromatic	450–800
8 Multispectral (Red, red edge, coastal, blue, green, yellow, near-IR1, and near-IR2)	400–1040
8 SWIR	1195–2365

1.1.2. Bathymetry data

Bathymetry data in the present research were collected using the Single Beam Echo Sounder (SBES) Bathy-2010 SyQwest instrument from March 20 to March 22, 2019 (Figure 1). Real-time positioning utilized the *Global Navigation Satellite System* (GNSS) Trimble NET R9 with a simple method. The data were acquired at the beginning of the survey. The main lane width was 20 meters and then subsequently adjusted to 50 m depending on the survey area and time. Figure 1 presents a ship route map for bathymetric survey and field documentation in Karimunjawa waters, Central Java.

This research employed data with a depth of 0 to 20 meters. The depth was then grouped into four groups, ranging from 0–5 meters, 5–10 meters, 10–15 meters, and 15–20 meters (Table 2). When acquiring depth data in shallow waters and water areas with lots of coral reefs, the vessel's limitation means that the depth of <2 meters is not well acquired. It is represented by the range of 0–5 meters. In this research, the depth data that was used for modeling were corrected due to tidal effect at first. The acquisition process was carried out during the day because the tides could affect the measured depth. Depth data were also corrected for transducer offset.

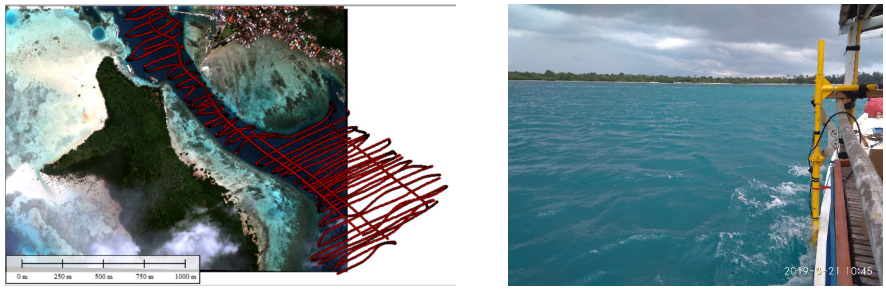

Figure 1. Ship route map for bathymetric survey and field documentation (source: Basith & Prastyani, 2020)

Table 2. The sample depth in this research

Depth (meters)	Total	Average (meters)	Standard Deviation (meters)
0–5	61	3,359	0,831
5–10	161	7,618	1,387
10–15	207	12,975	1,403
15–20	204	16,488	1,095

1.1.3. Field data

a) Spectral field

This research uses validated data using field spectral data that has been conducted by (Nuha, 2019). The measurement used the TriOS Ramses Spectrometer and its position was determined using GNSS with the absolute method. TriOS Ramses has a relatively small size and low power consumption. Therefore, the device is deemed very flexible to acquire data in the field. The device combines hyperspectral light measurement with maximum flexibility with its modular system. It was carried out at four stations/research locations. The location represented different water conditions, such as clear and cloudy. Table 3 provides the coordinate point of the location for water attenuation in Karimunjawa waters, Central Java (Nuha, 2019).

Table 3. Location of field spectral station (*water attenuation*) (source: Nuha, 2019)

Station	λ	φ	Water Condition
Station 1	–5.885740	110.439960	Cloudy
Station 2	–5.879454	110.428316	Cloudy
Station 3	–5.864106	110.420920	Clear
Station 4	–5.864106	110.413442	Clear

Nuha (2019) has been processing and combining 48 depth data were recorded synchronous to the spectral data, both positive and negative. It should be noted that the SDB Semi-Analytical model only uses data with positive values. Data with negative values cannot be used for model building. Having sorted, the research found 25 negative values. Thus, the formation of a semi-analytical model in this research used 23 positive data.

b) Water constituent

Supporting data for water constituents were obtained during the bathymetry survey from March 20 to March 22, 2019 by Nuha (2019). This data is additional one that describes the condition of the waters in the SDB analysis. The measurement of water constituents includes *Chlorophyll, Color Dissolved Organic Matter* (CDOM), *Total Suspended Solid* (TSS), and *Total Organic Matter* (TOM). Chlorophyll, CDOM, TSS, and TOM data were analyzed in the laboratory in 2019 by (Nuha, 2019).

Table 4 shows that the highest TSS contents were located at locations 2 and 4. These locations had a higher level of turbidity than other sampling locations. Meanwhile, the highest chlorophyll content was documented at location 3, followed by the relative TOM, CDOM, and TSS content. This location is located near the Karimunjawa port so that community activity on land might affect the turbidity level and water content. In the SDB technique, the condition of the waters' optical properties can affect the weakening process of electromagnetic waves. The following table presents the results of the water constituent content at four stations in the southern waters of Karimunjawa, Central Java (Nuha, 2019).

Table 4. Constituent content at four locations (source: Nuha, 2019)

Location	TOM (%)	CDOM	Chlorophyll (µg/l)	TSS (mg/ l)
Location 1	99.71	0.001	0.192	5.2
Location 2	99.69	0.001	0.116	10.0
Location 3	99.76	0.002	0.510	9.6
Location 4	99.77	0.002	0.273	12.0

1.2. Methods

1.2.1. Semi-analytical method

The semi-analytical method is the development of an analytical method. In this method, estimating the depth value and field parameters are considered in the measurement. Dual-channel equations are formed using two wavelengths contained in the image. Benny and Dawson (1983), Su et al. (2008) illustrate Dual-channel equations as follows:

$$Z = \left[\frac{1}{f_{(k2-k1)}}\right]\left[\ln\left(\frac{C_1 R_{b1}}{C_2 R_{b2}}\right) - \underbrace{\mathrm{Ln}(L_1 - L_{s_1})}_{X_1} + \underbrace{\mathrm{Ln}(L_2 - L_{s_2})}_{X_2}\right], \quad (1)$$

where: $k1$ – diffusion coefficient of 1st channel attenuation; $k2$ – diffusion coefficient of 2nd channel attenuation; C_1 – solar radiation constant, atmosphere, and water transmittance of channel 1; C_2 – solar radiation constant, atmosphere, and water transmittance of channel 2; R_{b1} – 1st channel reflectance substrate; R_{b2} – 2nd channel reflectance substrate; L_1 – 1st channel light; L_2 – 2nd channel light; Ls_1 – 1st channel light in the water; Ls_2 – 2nd channel light in the water.

Then, Equation (1) can be simplified into the following equation (Benny & Dawson, 1983; Su et al., 2008):

$$Z = A_0 + A_1 X_1 + A_2 X_2, \quad (2)$$

where: Z – the estimated value of the water depth of the 1st and 2nd channel combinations; X_1 – 1st channel pixel value; X_2 – 2nd channel pixel value; A_0 – constant; A_1 – channel gradient coefficient to 1; A_2 – 2nd channel gradient coefficient.

1.2.2. Polynomial regression

Regression is a statistical analysis that aims to see the relationship between the depth value of pixel extraction and

the measured depth value. The SDB technique generally uses this analysis to see the best correlation between the linked variables in model building. Polynomial regression was used if the field spectral data was not linear with measured depth data, usually marked with a curve (Nuha, 2019). The Polynomial regression can be mathematically expressed by the following equation (Mishra et al., 2006):

$$y = a + bx + cx^2 + dx^3 + ..., \quad (3)$$

where: y – the value of the depth of the SBES measurement ($a = m1$, $b = m2$, $c = m3$); x – the SDB value up to the next order point.

1.2.3. Accuracy test

a) The Root Mean Square Error (RMSE)

Ghilani (2010) stated that every measurement must have an error. For that reason, an accuracy test is necessary. As this research employed the semi-analytical method, a spectral measurement was performed to form a model, which was then applied to satellite images. *The Root Mean Square Error* (RMSE) equation is calculated as follows (Manessa et al., 2017; Walpole, 1968):

$$RMSE = \sqrt{\frac{\sum_{t=1}^{n}(At - Ft)^2}{n}}, \quad (4)$$

where: At – the estimated value of the depth from the image pixel value extraction; Ft – the measured depth of the survey results with the SBES; N – the number of depth points measured.

b) Total Vertical Uncertainty (TVU)

The use of the SDB method to estimate the depth of shallow seas requires a precision test with a predetermined standard. It commonly refers to the International Hydrographic Organization (IHO). The following is an equation for the TVU accuracy test (Gao, 2010; Mather, 2004):

$$TVU_{\max}(d) = \sqrt{a^2 + (b \times d)^2}, \quad (5)$$

where: a – represents that portion of the uncertainty that does not vary with the depth; b – a coefficient which represents that portion of the uncertainty that varies with the depth; d – the depth.

2. Results and discussion

2.1. Dual-Channel modelling

The model is formed using the relationship between the reflectance value of the field measurement results and the measured depth data. The reflectance parameters were symbolized as B2, B3, and B5 representing Blue, Green, and Red channels. The input data involved 23 positive data where the depth recording time and the water attenuation (spectral field) were synchronous (Nuha, 2019).

All input data created a non-linear function, as evidenced by a warped curve. Therefore, the formation of a dual-channel model used Multiple Polynomial Regression analysis degrees 1 and 2. The dual-channel method produces 12 models using visible spectrum red, green, and blue. The following table of models resulted from a combination of the Worldview 3 visible spectrum.

Table 5. The combinations of blue and green channels

Model	Std. Error of the Estimate	Model Equations
Model 1	2.77446978	$\beta_0 + \beta_1$ Blue + β_2 Green + ε
Model 2	2.55291434	$\beta_0 + \beta_1$ Blue + β_2 Green + β_3 Blue^2 +ε
Model 3	2.43523371	$\beta_0 + \beta_1$ Blue + β_2 Green + β_3 Green^2 +ε
Model 4	2.37743011	$\beta_0 + \beta_1$ Blue + β_2 Green + β_3 Blue^2 + β_4 Green^2 + ε

The Table 5 shows that the combination of blue and green channels produces the value of Std. Error of the Estimate is smaller than other channel combinations. Table 5 shows that model 4 is the best model with the equation $\beta_0 + \beta_1$ Blue + β_2 Green + β_3 Blue^2 + β_4 Green^2 + ε. The blue and green channels have a lower light spectrum absorption rate than other channels in water objects so that the light penetration can penetrate the water column deeper. At the same time, model 1 in Table 5 with the equation $\beta_0 + \beta_1$ Blue + β_2 Green + ε produces the value of Std. Error of the Estimate is bigger than others.

Table 6. The combinations of blue and red channels

Model	Std. Error of the Estimate	Model Equations
Model 1	3.38308383	$\beta_0 + \beta_1$ Blue + β_2 Red + ε
Model 2	3.03117469	$\beta_0 + \beta_1$ Blue + β_2 Red + β_3 Blue^2 +ε
Model 3	2.92896824	$\beta_0 + \beta_1$ Blue + β_2 Red + β_3 Red^2 +ε
Model 4	2.99276336	$\beta_0 + \beta_1$ Blue + β_2 Red + β_3 Blue^2 + β_4 Red^2 + ε

Table 6 shows that the combination of blue and red channels produces Std. The error of the Estimate is bigger than the blue and green channels. The spectrum in the red channel has a high absorption rate in water objects so that the spectrum is completely absorbed. These factors make the dual-channel model not optimal when using the red channel. Then the channel combination in Table 7 shows the value of Std. The error of the Estimate is bigger than the blue and green channels. The model with the red channel produces low accuracy.

Table 7. The combinations of green and red channels

Model	Std. Error of the Estimate	Model Equations
Model 1	3.29494874	$\beta_0 + \beta_1$ Green + β_2 Red + ε
Model 2	2.69256753	$\beta_0 + \beta_1$ Green + β_2 Red + β_3 Green^2 +ε
Model 3	2.87074069	$\beta_0 + \beta_1$ Green + β_2 Red + β_3 Red^2 +ε
Model 4	2.76392781	$\beta_0 + \beta_1$ Green + β_2 Red + β_3 Green^2 + β_4 Red^2 + ε

Twelve models were generated using the two-channel method, the three best models were applied to Worldview 3 imagery for depth estimation using 0–20 meter depth sample data. Determination of the best model was done by examining the value of Standard Error of the Estimate resulting from statistical analysis. The smaller the value of Standard Error of the Estimate, the better the resulting model.

The first best model was the equation $\beta_0 + \beta_1$ Blue + β_2 Green + β_3 Blue^2 + β_4 Green^2 + ε with the value of Std. Error of the Estimate is 2.377 meters. Table 8 shows the results of coefficients values generated from the regression analysis, the above equation can be rewritten as 6.334 + 1649.644 blue – 1624.194 green – 17 788.594 blue^2 + 15069.410 green^2 + ε. Then, for depth estimation, the model was applied to the image using the band match feature in the ENVI software. The definition of the model above can be written as 6.334 + 1649.644 × B2 – 1624.194 × B3 – 17788.594 × B2^2 + 15069.410 × B3^2, where B2 denotes Blue and B3 is Green.

The second best model constituted the equation $\beta_0 + \beta_1$ Blue + β_2 Green + β_3 Green^2 +ε with the value of Std. Error of the Estimate is 2,435 meters. Table 8 shows the results of coefficients values generated from the regression analysis, the above equation can be expressed by 8.534 + 866.573 blue – 1130.525 green + 4751.793 green^2 + ε. For depth estimation, the model was then applied to the image using the same feature from the ENVI software. Further, the definition of the model can be illustrated as 8.534 + 866.573 × B2 – 1130.525 × B3 + 4751.793 × B3^2, where B2 indicates Blue and B3 is Green.

The third best model was the equation $\beta_0 + \beta_1$ Blue + β_2 Green + β_3 Blue^2 +ε with the value of Std. Error of the Estimate is 2,553 meters. Table 8 shows the results of coefficients values from the regression analysis, the above equation can be rewritten as 8.797 + 585.464 Blue – 905.041 Green + 6809.984 Blue^2 + ε. Then, for depth estimation, the model was applied to the image using the same software feature as above. The definition of the model can be expressed by 8.797 + 585.464 × B2 – 905.041 × B3+ 6809.984 × B2^2 + ε, where B2 is Blue and B3 represents Green.

Table 8. Coefficients values of the best regression models

Model	Model 1 (B)	Model 2 (B)	Model 3 (B)
(Constant)	6.334	8.534	8.797
Blue	1649.644	866.573	585.464
Green	–1624.194	–1130.525	–905.041
Blue^2	–17788.594	–	6809.984
Green^2	15069.410	4751.793	–

2.2. Depth estimation results

First, at a depth of 0 to 5 meter, the model with the equation $\beta_0 + \beta_1$ Blue + β_2 Green + β_3 Blue2 + β_4 Green2 + ε were reported to produce an RMSE value of 2,102 meters. At a depth of 0–5 meters, the RMSE generated using the Semi-Analytical method tends to be large. It was reported that one data were included in the particular order class IHO, one data were included in the order of class 1A / 1B, and two data were included in the order of class 2. At that depth, only a few depth data that meet IHO standards.

Second, the accuracy-test was carried out at a depth of 5–10 meters. The model with the equation $\beta_0 + \beta_1$ Blue + β_2 Green + β_3 Blue^2 + β_4 Green^2 + ε produced the best depth estimation that was indicated by the RMSE value of 1,592 meters. The model generated a depth estimate value that was included in the IHO standards. It was reported that 12 data (8.39%) were included in the particular order class, 17 data (11.89%) were included in the order of class 1A / 1B, and 27 data (18.88%) were included in the order of class 2.

Third, the accuracy-test was also performed at a depth of 10–15 meters. The best model with the equation $\beta_0 + \beta_1$ Blue + β_2 Green + β_3 Green^2 +ε produced an RMSE value of 2,099 meters. The model generated a depth estimation value that was included in the IHO standard, covering 12 data (5.80%) included in the particular order, 16 data (7.73%) included in the order of class 1A / 1B, and 23 data (11.11%) fell into the second-order class IHO. Fourth, the accuracy-test was conducted at a depth of 15–20 meters. The model with the equation $\beta_0 + \beta_1$ Blue + β_2 Green + β_3 Green^2 +ε yielded the best depth estimation as shown by the RMSE value of 1,239 meters. The model produced a depth value following the IHO standard. The results revealed that 44 data (21.57%) were categorized in the particular order class, 64 data (31.37%) fell into the order of class 1A / 1B, and 90 data (44.12%) were included in the order of class 2.

In short, this research shows that the dual-channel, semi-analytical method is better in estimating the depth value at the depth interval 5 to 20 meters. Meanwhile, at a depth of 0 to5 meters, the two-channel semi-analytical model produces a sizeable RMSE value. The use of dual-channel is effective in water depth of 5 to 20 meters because, in estimating the depth, the light spectrum with a high absorption will be covered with a low absorption rate spectrum. The research also finds out that there are still models that meet the IHO standard criteria ([6.334 + 1649.644×B2 – 1624.194 × B3 – 17788.594 × B2^2 + 15069.410 × B3^2 at a depth of 5–10 meters], and [8.534 + 866.573 × B2 – 1130.525 × B3 + 4751.793 × B3^2 at a depth of 10 to 20 meters]).

The research using semi-analytical methods was conducted by Nuha (2019) using the one-channel model. The study showed the yellow channel with the exponential model produces 39.59% data were categorized in the particular order class, 47.72% data fell into the order of class 1A/1B, and 54.31% data were included in the order of class 2. The semi-analytical method's dual-channel model produces a better depth estimate than the single-channel, especially at a depth of 5 to 20 meters.

Conclusions

In conclusion, this research has shown that the proposed model ([6.334+1649.644×B2 – 1624.194×B3 – 17788.594×B2^2 + 15069.410×B3^2] and [8.534 + 866.573×B2 – 1130.525×B3 + 4751.793×B3^2]) has been confirmed to improve the depth accuracy. The spectral value of the waters which are measured directly in the field (water attenuation) and used in the formation of semi-analytical models has been shown to increase the depth estimation results. The research also indicates that the use of dual-channel can complement each other in the estimation process. Channels with high absorption rates in the water column will be covered with channels that have low absorption rates. The blue and green channels in the Worldview 3 image are the best models, especially for estimating depths with interval from 5 to 20 meters. The wavelengths in the two channels have a low absorption rate to penetrate deeper waters compared to other wavelengths.

Acknowledgements

The authors would like to thank Universitas Gadjah Mada and the Department of Geodesy Engineering - Engineering Faculty for providing financial assitance for this research.

Funding

This research was supported by a research grant from the Department of Geodesy (No. 231.j/H1.17/ TGD/PL/2019), Community Research Program, and the RTA of Universitas Gadjah Mada, Indonesia.

Author contributions

Abdul Basith was responsible for data acquisition and design of data analysis and was supervisor of Nuha (2019). In addition, Luhur Moekti Prayogo contributed to forming dual-channel model using semi-analytical methods. Gathot Winarso and Kuncoro Teguh Setiawan was responsible for data acquisition and analysis of field spectral.

References

Basith, A., & Prastyani, R. (2020). Evaluating acomp, flaash and quac on worldview-3 for satellite derived bathymetry (SDB) in shallow water. *Geodesy and Cartography*, *46*(3), 151–158. https://doi.org/10.3846/gac.2020.11426

Benny, A. H., & Dawson, G. J. (1983). Satellite imagery as an aid to bathymetric charting in the red sea. *Cartographic Journal*, *20*(1), 12. https://doi.org/10.1179/caj.1983.20.1.5

Bierwirth, P. N., Lee, T. J., & Burne, R. V. (1993). Shallow seafloor reflectance and water depth derived by unmixing multispectral imagery. *Photogrammetric Engineering and Remote Sensing*, *59*(3), 331–338.

Bramante, J. F., Raju, D. K., & Sin, T. M. (2013). Multispectral derivation of bathymetry in Singapore's shallow, turbid waters. *International Journal of Remote Sensing*, *34*(6), 37–41. https://doi.org/10.1080/01431161.2012.734934

Collet, C., Provost, J. N., Rostaing, P., Pérez, P., & Bouthemy, P. (2000). Spot satellite data analysis for bathymetric mapping. *IEEE International Conference on Image Processing* (pp. 464–467). IEEE. https://doi.org/10.1109/ICIP.2000.899440

Danoedoro, P. (2012). *Introduction to digital remote sensing* (1st ed.). ANDI Publisher.

Dierssen, H. M., Zimmerman, R. C., Leathers, R. A., Downes, T. V., & Davis, C. O. (2003). Ocean color remote sensing of seagrass and bathymetry in the Bahamas Banks by high-resolution airborne imagery. *Limnology and Oceanography*, *48*, 444–455. https://doi.org/10.4319/lo.2003.48.1_part_2.0444

Gao, J. (2009). Bathymetric mapping by means of remote sensing: Methods, accuracy and limitations. *Progress in Physical Geography*, *33*(1), 103–116. https://doi.org/10.1177/0309133309105657

Gao, J. (2010). *Digital Analysis of remotely sensed imagery*. McGrawHill.

Garlan. (1989). *Spatial cartography of the Coralline coast: Topography and bathymetry.* Service Hydrographique et Oceanographique de la Marine, Ministere de la Defense.

Ghilani, C. D. (2010). *Adjustment computations: Spatial data analysis*. Wiley. https://doi.org/10.1002/9780470586266

Hidayah, Z., Prayogo, L. M., & Wardhani, M. K. (2018). Sea level rise impact modelling on small islands: Case study Gili Raja island of east Java. *MATEC Web of Conferences*, *177*, 01017. https://doi.org/10.1051/matecconf/201817701017

Jupp, D. L. B. (1989). Background and extensions to depth of penetration (DOP) mapping in shallow coastal waters. In *Proceedings of Remote Sensing of the Coastal Zone International Suposium* (pp. IV.2.1–IV.2.19).

Karimi, N., Bagheri, M. H., Hooshyaripor, F., Farokhnia, A., & Sheshangosht, S. (2016). Deriving and evaluating bathymetry maps and stage curves for shallow lakes using remote sensing data. *Water Resources Management*, *30*, 5003–5020. https://doi.org/10.1007/s11269-016-1465-9

Lafon, V., Froidefond, J. M., Lahet, F., & Castaing, P. (2002). SPOT shallow water bathymetry of a moderately turbid tidal inlet based on field measurements. *Remote Sensing of Environment*, *81*(1), 136–148. https://doi.org/10.1016/S0034-4257(01)00340-6

Leu, L. G., & Chang, H. W. (2005). Remotely sensing in detecting the water depths and bed load of shallow waters and their changes. *Ocean Engineering*, *32*, 1174–1198. https://doi.org/10.1016/j.oceaneng.2004.12.005

Lyzenga, D. R. (1978). Passive remote sensing techniques for mapping water depth and bottom features. *Applied Optics*, *17*(3), 379–383. https://doi.org/10.1364/AO.17.000379

Lyzenga, D. R. (1985). Shallow-water bathymetry using combined lidar and passive multispectral scanner data. *International Journal of Remote Sensing*, *6*, 15–125. https://doi.org/10.1080/01431168508948428

Manessa, M. D. M., Haidar, M., Hartuti, M., & Kresnawati, D. K. (2017). Determination of the best methodology for bathymetry mapping using spot 6 imagery: A study of 12 empirical algorithms. *International Journal of Remote Sensing and Earth Sciences (IJReSES)*, *4*(2), 127–136. https://doi.org/10.30536/j.ijreses.2017.v14.a2827

Martin, S. (2014). *An introduction to ocean remote sensing*. Cambridge University Press. https://doi.org/10.1017/CBO9781139094368

Mather, P. M. (2004). *Computer processing of remotely sensed data: An introduction.* (3 ed.). John Wiley and Sons.

Mishra, D., Narumalani, S., Rundquist, D., & Lawson, M. (2006). Benthic habitat mapping in tropical marine environments using quickbird multispectral data. *Photogrammetric Engineering and Remote Sensing*, (9), 1037–1048. https://doi.org/10.14358/PERS.72.9.1037

Misra, A., Vojinovic, Z., Ramakrishnan, B., Luijendijk, A., & Ranasinghe, R. (2018). Shallow water bathymetry mapping using Support Vector Machine (SVM) technique and multispectral imagery. *International Journal of Remote Sensing*, *39*(13), 4431–4450. https://doi.org/10.1080/01431161.2017.1421796

Nuha, M. U. (2019). *Optimization of ocean depth extraction analytical parameters with high resolution satellite imagery in the shallow sea zone* [PhD Thesis]. Universitas Gadjah Mada, Yogyakarta, Indonesia.

Prayogo, L. M., & Basith, A. (2020). Image performance test on Worldview 3 and sentinel 2A for mapping shallow water depth (case study in Karimunjawa Islands, Central Java). *JGISE: Journal of Geospatial Information Science and Engineering*, *3*(2), 161–167. https://doi.org/10.22146/jgise.59572

Provost, J. N., Collet, C., Perez, P., & Bouthemy, P. (1999). Hierarchical unsupervised multispectral model to segment SPOT images for ocean cartography. In *IEEE International Conference on Image Processing* (pp. 333–337). IEEE. https://doi.org/10.1109/ICIP.1999.821625

Sánchez-Carnero, N., Ojeda-Zujar, J., Rodríguez-Pérez, D., & Marquez-Perez, J. (2014). Assessment of different models for bathymetry calculation using SPOT multispectral images in a high-turbidity area: The mouth of the Guadiana Estuary. *International Journal of Remote Sensing*, *35*(2), 493–514. https://doi.org/10.1080/01431161.2013.871402

Satellite Imaging Corporation. (2020, January 18). *Worldview-3 Band Spesifications*. https://www.satimagingcorp.com/

Stumpf, R. P., Holderied, K., Robinson, J. A., Feldman, G., & Kuring, N. (2003a, July 13–17). Mapping water depths in clear water from space. In *Proceedings of the 13th Biennial Coastal Zone Conference Baltimore*.

Stumpf, R. P., Holderied, K., & Sinclair, M. (2003b). Determination of water depth with high-resolution satellite imagery over variable bottom types. *Limnology and Oceanography*, *48*(1), 547–556. https://doi.org/10.4319/lo.2003.48.1_part_2.0547

Su, H., Liu, H., & Heyman, W. (2008). Automated derivation of bathymetric information from multi-spectral satellite imagery using a non-linear inversion model. *Marine Geodesy*, *31*(4), 281–298. https://doi.org/10.1080/01490410802466652

Sutherland, J., Walstra, D. J. R., Chesher, T. J., van Rijn, L. C., & Southgate, H. N. (2004). Evaluation of coastal area modelling systems at an estuary mouth. *Coastal Engineering*, *51*(2), 119–142. https://doi.org/10.1016/j.coastaleng.2003.12.003

Walpole, R. E. (1968). *Introduction to statistics*. Macmillan.